FULL-LENGTH ORIGINAL RESEARCH

Ictal perfusion changes associated with seizure progression in the amygdala kindling model in the rhesus monkey

*†Evy Cleeren, ‡§Cindy Casteels, ‡Karolien Goffin, *Peter Janssen, and †Wim Van Paesschen

Epilepsia, **(*):1–10, 2015
doi: 10.1111/epi.13077

Summary

Objective: Amygdala kindling is a widely used animal model for studying mesial temporal lobe epileptogenesis. In the macaque monkey, electrical amygdala kindling develops slowly and provides an opportunity for investigating ictal perfusion changes during epileptogenesis.

Methods: Two rhesus monkeys were electrically kindled through chronically implanted electrodes in the right amygdala over a period of 16 and 17 months. Ictal perfusion single photon emission computed tomography (SPECT) imaging was performed during each of the four predefined clinical stages.

Results: Afterdischarge duration increased slowly over 477 days for monkey K and 515 days for monkey S (18 ± 8 s in stage I; 52 ± 13 s in stage IV). During this time, the animals progressed through four clinical stages ranging from interrupting ongoing behavior to bilateral convulsions. Ictal SPECT perfusion imaging showed well-localized but widely distributed regions of hyperperfusion and hypoperfusion, in both cortical and subcortical structures, at every seizure stage. A large portion of the ictal network was involved in the early stages of epileptogenesis and subsequently expanded over time as seizure severity evolved.

Significance: Our data indicate that the different mesial temporal lobe seizure types occur within a common network affecting several parts of the brain, and that seizure severity may be determined by seizure-induced epileptogenesis within a bihemispheric network that is implicated from the start of the process.

KEY WORDS: Amygdala kindling, Rhesus monkey, Epileptogenesis, Single photon emission computed tomography.

Evy Cleeren is a doctoral student at the KU Leuven.

Temporal lobe epilepsy (TLE) is the most common form of focal epilepsy.[1] Little is known about how a healthy brain transforms into an epileptic brain, a process called epileptogenesis.[2] Most of our understanding about epileptogenesis and epilepsy comes from animals models in rodents.[3] Only a few animal studies concerning epileptogenesis have been conducted in nonhuman primates.[4–8]

Electrical kindling of the amygdala has been proposed as a model for mesial temporal lobe epileptogenesis. Electrical kindling is defined as the phenomenon whereby repeated administration of an initially subconvulsive electrical stimulus results in progressive intensification of seizure activity, culminating in a generalized seizure.[9] Kindling progresses slowly over time, depending on the species used. For example, on average, 18 and 25 stimulations are necessary to evoke a generalized seizure in Wistar rats and cats, respectively.[10] Furthermore, spontaneous seizures are rare, making this model suitable for longitudinal, well-controlled studies.

Ictal perfusion single photon emission computed tomography (SPECT) is an imaging technique used to localize the seizure-onset zone during the presurgical evaluation of patients with refractory epilepsy.[11] Ictal perfusion SPECT has also been used to study widespread changes in brain

Accepted June 10, 2015.

*Laboratory for Neuro- and Psychophysiology, KU Leuven, Leuven, Belgium; †Laboratory for Epilepsy Research, KU Leuven, Leuven, Belgium; ‡Nuclear Medicine & Molecular Imaging, Department of Imaging and Pathology, KU Leuven, Leuven, Belgium; and §Molecular Small Animal Imaging Center (MoSAIC), KU Leuven, Leuven, Belgium

Address correspondence to Wim Van Paesschen, Laboratory for Epilepsy Research, UZ Herestraat 49 Box 7003, 3000 Leuven, Belgium. E-mail: wim.vanpaesschen@uzleuven.be

Wiley Periodicals, Inc.

Key Points

- The amygdala kindling model in the rhesus monkey is a good model to study mesial temporal epileptogenesis.
- The ictal network during kindling epileptogenesis was extended bi-hemispherically from the start of the process and involved regions of hyperperfusion and hypoperfusion.
- Changes in the ictal perfusion network during kindling arose mainly from this early common network.

perfusion during seizures. Complex focal seizures in mesial temporal lobe epilepsy with hippocampal sclerosis (MTLE-HS) are associated with hyperperfusion in the ipsilateral temporal lobe, middle frontal and precentral gyrus, bilateral occipital lobes, and the contralateral postcentral gyrus, whereas hypoperfusion was observed in both frontal lobes, the contralateral cerebellum, and the ipsilateral precuneus.[12] A recent study employing resting state functional MRI (fMRI) in patients with MTLE revealed increased hippocampal connectivity in similar regions.[13]

Wada et al.[5] were the first to describe electroclinical changes in the kindling model in rhesus monkeys. They showed a very slow increase in seizure duration and severity over the course of about 400 days of stimulation, ranging from interrupting ongoing activity during a stage I seizure to secondarily generalized tonic–clonic seizures with marked asymmetry in stage IV. In the present study, we wanted to capitalize on the gradual progression of kindling in the rhesus monkey to investigate changes in brain perfusion during epileptogenesis. Moreover, ictal SPECT imaging during amygdala kindling in the monkey provides the additional advantage in that the time of seizure onset and thus tracer injection is exactly controlled.

Materials and Methods

Animals and surgery

All experiments were performed using two male rhesus monkeys (*Macaca mulatta*; adult monkey K: 9 kg, juvenile monkey S: 6 kg, both housed socially) who were trained to sit in a primate chair. A head post (Crist Instrument) was implanted on the skull using ceramic screws and dental acrylic. All surgical procedures were performed under isoflurane anesthesia (1%) and strict aseptic conditions. A custom-made bundle of microelectrodes (seven in monkey S, three in monkey K; tungsten, 125 μm diameter, impedance at 1 kHz: 130 kΩ; Frederick Haer Company (FHC)) was chronically implanted in the right amygdala (Horsley-Clarke coordinates 22A-9L for monkey K; 17A-9L for monkey S) based on preoperative structural magnetic resonance (MR) images. One of these electrodes was used for electrical stimulation, and a second (located approximately 1–2 mm from the stimulation electrode) was used for depth electroencephalography (EEG) recording. During the same surgery, a low-impedance (<10 kΩ) reference electrode was inserted into the white matter of the frontal lobe. Electrically stimulating an amygdala electrode using this low-impedance reference will result in a high charge density in the amygdala. In addition, four titanium screws (Synthes) were inserted in the skull for epidural EEG recording bilaterally over the frontal and occipital lobe. Postoperatively, the location of the electrodes was verified by a T_1-weighted anatomic MR image (0.4 mm isotropic resolution, TIM Trio; Siemens Healthcare). The tip of the stimulation

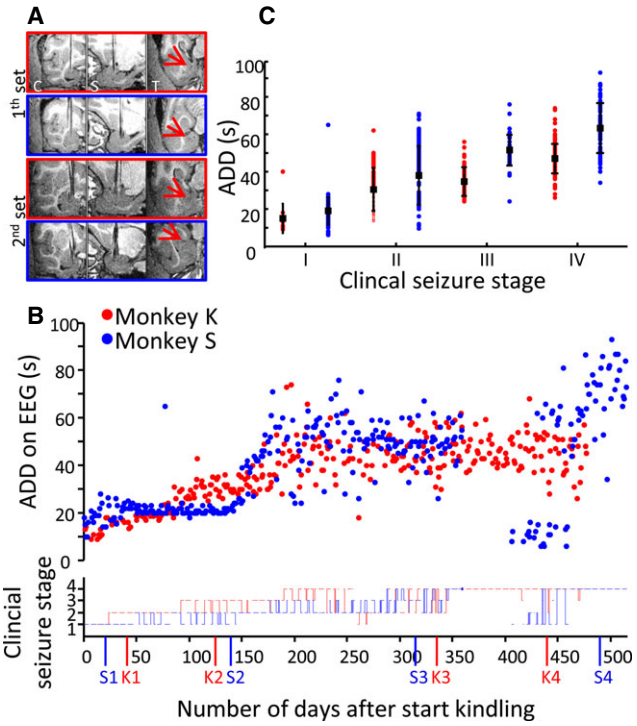

Figure 1.
Kindling progression over time. (**A**) Stimulation sites. Coronal, sagittal, and transverse MR images showing the location of the electrodes (arrows) in the right amygdala in each animal; the upper two rows show the initial positions in monkey K (red) and monkey S (blue), and the bottom two rows show the positions after replacement. C, coronal section; S, sagittal section; T, transverse section. (**B**) The progression of the duration of the afterdischarge (ADD) as measured on the amygdala EEG as a function of time and in relation to clinical stage. Daily stimulation of the amygdala showed a stepwise increase in seizure duration and a progression throughout the various clinical stages. The chronic electrodes were replaced after 258 days in monkey K and 367 days in monkey S. Electrical stimulation in monkey S with the new electrodes was resumed at day 406. Extra annotations on the *x*-axis denote the timing of the ictal SPECT scans. (**C**) Variation in ADD as a function of the seizure stage. Black line depicts mean ± SD.

electrode was located in or near the basomedial amygdaloid nucleus in both animals (Fig. 1A). At least 6 weeks after implantation of the head post, monkeys were trained to perform a passive fixation task. All experimental procedures were performed in accordance with the National Institutes of Health Guide for the Care and Use of Laboratory Animals and EU Directive 2010/63/EU, and were approved by the ethical committee at the KU Leuven.

Amygdala kindling protocol

Daily electrical stimulation of the amygdala was begun 8 weeks (monkey K) and 13 weeks (monkey S) after implantation of the electrodes. On day 1 we determined the afterdischarge threshold (ADT) by administering stimulation pulses (duration: 1 s; 60 Hz sine wave) with increasing intensity (starting at 100 μA) until a localized afterdischarge appeared in the amygdala EEG (DS8000 digital stimulator/DLS100 digital linear stimulus isolator; World Precision Instruments). The ADT measured 1,100 μA for monkey K and 500 μA for monkey S. We electrically stimulated the amygdala once a day (between 8 and 12 a.m., 5 days a week) at this intensity. During these experiments, animals were monitored by video-EEG (Nicolet vEEG; Viasys Healthcare). Seizures were recorded with a high-definition camera. In addition, the animals performed a passive fixation task (fixation on a small spot on a display placed in front of the animal, for a liquid reward) to measure the postictal period. The position of the right eye was monitored by means of an infrared eye tracker (EyeLink1000; SR Research), and task performance was controlled by custom-built software running in LabView.

Kindled seizure activity was assessed using the following measurements: afterdischarge duration (ADD), clinical seizure severity, and duration of the postictal period. The duration of the afterdischarge was assessed by visual inspection of the EEG traces recorded in the amygdala. Seizure severity was classified according to Wada et al.[5]: (stage I) visual searching behavior; (stage II) oral automatisms; (stage III) unilateral convulsions; (stage IV) seizure generalization with marked asymmetry.

Brain perfusion imaging

^{99m}Tc-ECD SPECT image acquisition

Animals were scanned once at five different time points: a baseline SPECT scan was obtained 4–8 weeks after implantation of the electrodes and before kindling had begun, and ictal SPECT scans during each of the four clinical seizure stages (stages I–IV). Because of the unpredictability of seizure stage and seizure stage progression, ictal SPECT scans were planned after we considered the monkeys to be stable in a particular seizure stage. The exact timing of the scans is denoted in Figure 1B (S1-4, K1-4). SPECT scanning took place after overnight fasting. For each scan, the monkey was monitored by video-EEG, while an average of 192.4 MBq (range 85.1–244.2 MBq) 99m-Technetium labeled ethyl cysteinate diethylester (^{99m}Tc-ECD, synthesized on-site) was injected into the saphenous vein. A seizure was elicited 10 s after the tracer injection. We injected preictally, since ictal injection was technically difficult due to ictal limb movements. Forty minutes postinjection, the monkeys were sedated with a mixture of ketamine (Ketalar; Pfizer) and medetomidine (Domitor; Pfizer). At this time point, cerebral tracer concentrations are in steady state[14] and are not influenced by the anesthetic agents. Image acquisition and reconstruction are described in Data S1.

Image analysis

Images were analyzed using the subtraction ictal SPECT coregistered to MRI (SISCOM) technique[15] (for details, see Data S1). The SISCOM images were displayed as an overlay on the MR image at $z \geq +1.5$ and $z \leq -1.5$.[11]

We tested which brain regions were activated at each clinical stage using a conjunction analysis. The z-score difference images for the two monkeys independently were used to determine for each voxel whether this voxel showed perfusion changes of >1.5 SD in every clinical stage.

To determine changes in the perfusion network over the course of kindling, we defined volumes of interest (VOIs) based on the SISCOM images of stage IV for each monkey using the xjview toolbox (http://www.alivelearn.net/xjview8) in SPM8. A VOI was defined as a cluster of contiguous voxels (size >200 voxels) that showed an increase or decrease of >1.5 SD in perfusion in the stage IV SISCOM image, excluding those voxels that appeared in the conjunction image. These VOIs were then applied to the SPECT images after global scaling to the average activity within the brain and the percent change with respect to the baseline SPECT was calculated. Only the VOIs that showed a progressive monotonic increase (hyperperfusion clusters) or decrease (hypoperfusion clusters) in percent perfusion change over the four stages were taken into account. We repeated the same analysis on the clusters (size >200 voxels) of the common network to evaluate the relationship between the perfusion changes in these common network clusters and the functionally defined VOIs.

Results

General properties of amygdala kindling

We electrically stimulated the amygdala at the ADT in 358 sessions in monkey S and 344 sessions in monkey K. Both monkeys showed the gradual clinical progression from stage I until stage IV seizures as described by Wada et al.[5] Stage I seizures were observed from the first day of kindling and were characterized in both monkeys by an immediate startle response following the onset of stimulation, interruption of ongoing behavior (i.e., the fixation task), and saccadic eye movements, although in a sizeable proportion (53%)

of stage I seizures in monkey S, we observed an autonomic aura (i.e., mydriasis) without further clinical signs. In stage II, we observed oral automatisms in both monkeys, accompanied by gaze deviation to the contralateral hemifield in monkey S and saccadic eye movements in monkey K. Sporadically (1/123 in monkey S, and 15/103 of the stage II seizures in monkey K.), we observed a short postictal period (lasting 10 s in monkey S, and averaging 14 ± 7 s in monkey K), characterized by immobility except for eye movements, after which the fixation task was resumed. In stage III, the motor signs became prominent: more pronounced oral automatisms, retraction of the contralateral mouth (monkey K), eye blinking, and dystonic contralateral limb movements. In addition, both animals experienced a short postictal period (averaging 19 ± 8 s in 18% of the stage III seizures in monkey S and 19 ± 11 s in 20% in monkey K). Finally, stage IV seizures appeared which, in addition to the symptoms of stage III, included bilateral limb involvement, with dystonic and clonic movements in all four limbs. Monkey S also occasionally showed vocalizations. The postictal period (20 ± 12 s in 42% of the stage IV seizures in monkey S. and 26 ± 16 s in 91% in monkey K) occurred significantly more frequently than in stage III (Fisher's exact test, $p < 0.01$ for both monkeys), but both animals always resumed the fixation task after this period. Consistent with Wada et al.,[5] we did not observe any spontaneous seizures.

Due to a failure of the chronically implanted electrodes, we replaced the electrodes in both animals (after 20 stage IV seizures in monkey S, and after 34 stage IV seizures in monkey K). Although their location in the amygdala was not identical to those of the first set (Fig. 1A), the seizures elicited by stimulation in the new location were similar. These results illustrate that the precise anatomic location of the stimulation electrode in the amygdala was not critical for eliciting stage IV seizures.

We recorded EEG signals in the amygdala during every seizure using a microelectrode located approximately 1 mm from the stimulation electrode. The main change in EEG recording was observed in duration of the ictal period, not in the power-frequency spectra (Fig. S1). In Figure 1B, we plotted the AD duration in the amygdala for each stimulation session, together with the clinical seizure stage. In both animals, the AD duration increased significantly ($p < 0.0001$) over time until a plateau was reached after approximately 200 stimulation sessions. The increase in AD duration occurred in a step-wise fashion (Fig. 1B). The average (±SD) AD duration increased from 15 ± 8 s (monkey K) and 19 ± 7 s (monkey S) in stage I to 47 ± 8 s (monkey K) and 63 ± 13 s (monkey S) in stage IV (Fig. 1C). To quantify the effect of amygdala kindling over time, we calculated a linear regression analysis on the data of the first 300 days after start of kindling with *AD duration* as the dependent variable, *seizure stage* as continuous predictor, and *monkey* as a categorical variable. The effect of *clinical seizure stage* was highly significant ($p < 0.0001$), whereas the factor *monkey* was not significant ($p = 0.55$). Figure 1C shows the average and the range of AD durations for each monkey at each clinical seizure stage. Figure 1B,C illustrates the variability of the AD duration in the amygdala, particularly in stage IV (difference in variance between stage I and stage IV: $p < 0.001$ in monkey S and $p = 0.02$ in monkey K, Levene's test). The large variability in AD duration was reflected in the instability of the clinical seizure stage, since even after >400 stimulation sessions we occasionally observed stage I or stage II seizures (Fig. 1B).

We also recorded the epidural EEG from four screws attached to the skull (two frontal and two occipital, Fig. S1). In the course of stage I, epileptic activity began to appear in these screw electrodes during the second half of a seizure (Fig. S2). From stage II onward, the EEG recorded from the screw electrodes also showed seizure activity, starting and ending together with the seizure activity recorded in the amygdala. A gradual propagation of seizure activity after amygdala stimulation could not be observed in these EEG recordings, which is most likely due to the small spatial sampling of electrodes.

Overall, we replicated the key features of amygdala kindling in the rhesus monkey as described by Wada et al.[5] In addition, the implementation of a task demonstrated that the postictal period, in which the animals were unable to perform the fixation task, increased in frequency over time but remained limited in time.

Brain perfusion changes during amygdala kindling

Individual and conjunction SISCOM images

An overview of SISCOM images for the four seizure stages in the two monkeys is displayed in Figure 2. In seizure stage I, the individual SISCOM images per monkey showed a distributed network of hyperperfusion and hypoperfusion regions (Fig. 2A,B, upper row). In this very early stage of the amygdala kindling process, where clinical manifestations were very subtle, both monkeys exhibited localized regions of hyperperfusion and hypoperfusion in throughout the cortex, and in many subcortical structures (cerebellum, basal ganglia, amygdala, and thalamus). Surprisingly, despite major behavioral and electrophysiologic changes that occurred over the course of the amygdala kindling process, the pattern of localized hyperperfusions and hypoperfusions remained similar across the stages II–IV. Although some regions showed hyperperfusion in all seizure stages (e.g., the amygdala in monkey S, and the insula in monkey K), other regions (e.g., the cerebellum) showed varying degrees of hyperperfusion and hypoperfusion.

Conjunction analysis (Fig. 3) showed that 6 ± 0.4% (monkey S) and 16 ± 1.1% (monkey K) of the hyperperfusion voxels, and 27 ± 1.8% (monkey S) and 27 ± 1.7% (monkey K) of the hypoperfusion voxels showed significant perfusion changes in all clinical stages. In both monkeys,

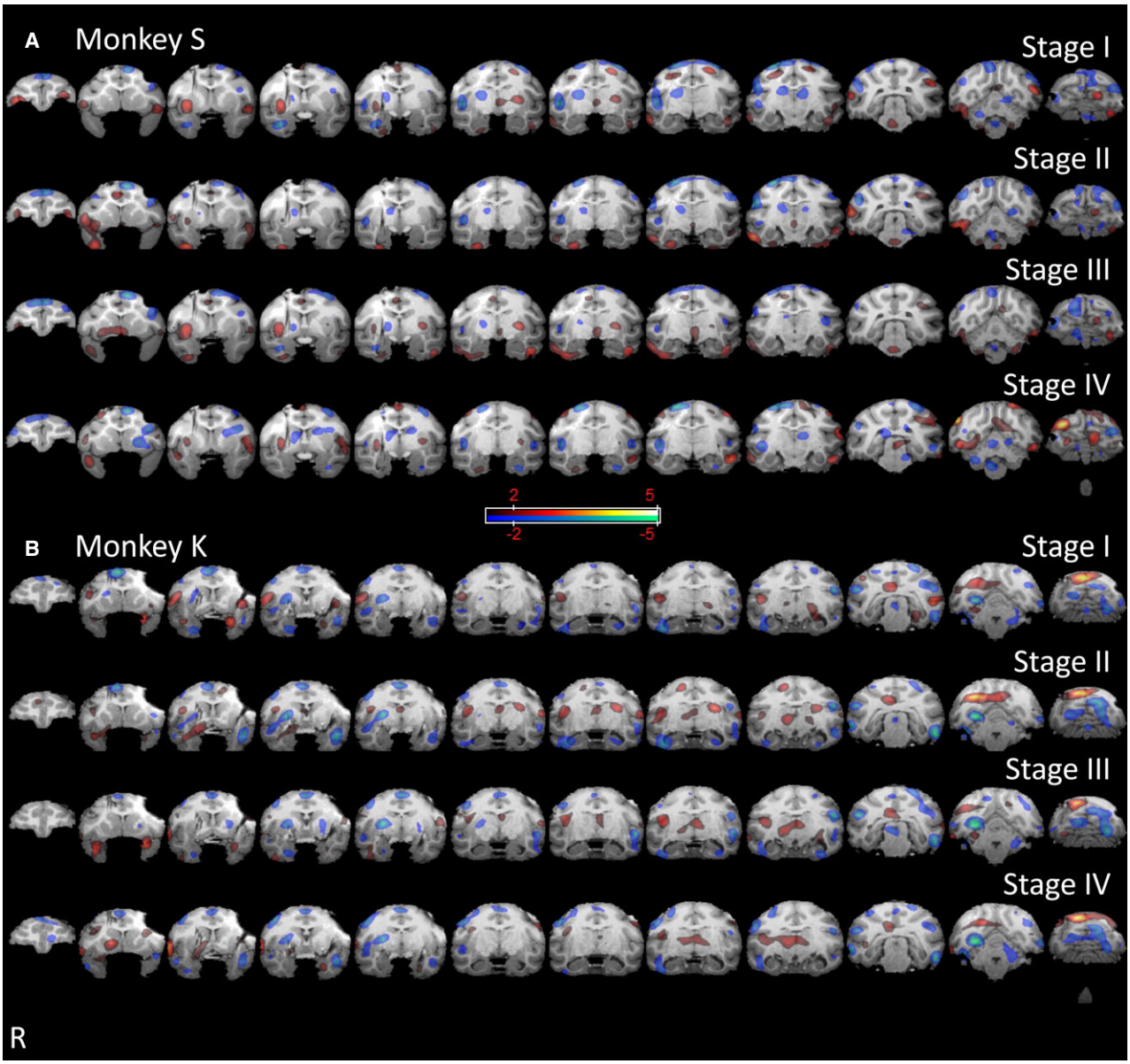

Figure 2.
SISCOM images. (**A**) Coronal brain sections showing the increase (red) and decrease (blue) in brain perfusion during a seizure as measured with ^{99m}Tc-ECD SPECT coregistered with the MRI for monkey S in the four different stages. Images are thresholded on 1.5 SD. Colorbar expresses z-scores. Left–right orientation is according to radiologic convention, right (R) is ipsilateral to stimulation side. (**B**) SISCOM images for monkey K. Same conventions as in **A**.

we measured hyperperfusion clusters that were common to all stages in both cortical (e.g., temporal and occipital) and subcortical structures (e.g., putamen and ventral amygdala in monkey S, thalamus in monkey K, Fig. 3). Similarly, regions showing hypoperfusion in all clinical seizure stages were localized but distributed across the brain (e.g., frontal cortex in both monkeys, basal ganglia in monkey K). A comparison of the results of the conjunction analyses in the two animals showed little overlap in the common networks of the two animals, most likely related to the subtle differences in clinical progression and in electrode location. Despite these interindividual differences, the conjunction analysis demonstrated that parts of the network activated during amygdala kindling were common to all clinical seizure stages in the individual monkeys.

Recruitment of brain regions during kindling

Next we investigated which brain regions were progressively recruited in the course of the four clinical seizure stages (Table 1 and Fig. 4). In both monkeys, we observed

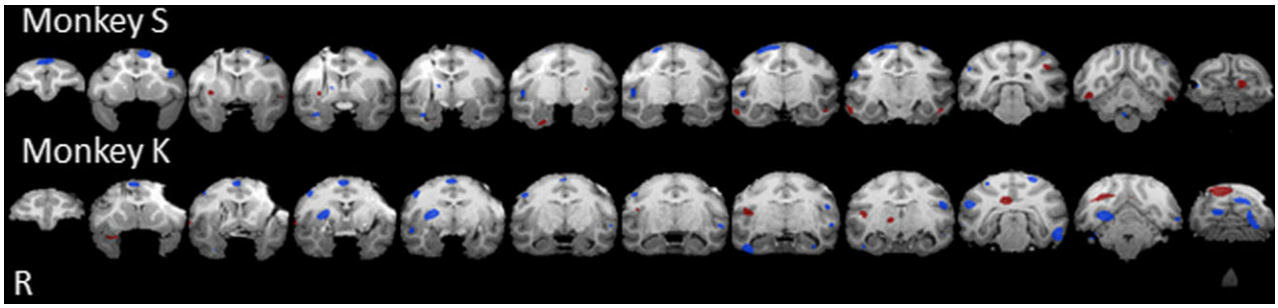

Figure 3.
Conjunction analysis on SISCOM images. Coronal brain sections depicting the hyperperfusion (red) and hypoperfusion (blue) clusters that show an increase or decrease at 1.5 SD in all four seizure stages. Same conventions and sections as in Figure 2.

regions with progressive increases in perfusion (12 in total; 8 in monkey S and 4 in monkey K), and progressive decreases in perfusion (8 in total; 4 in monkey S and 4 in monkey K).

We measured progressive hyperperfusion through the four seizure stages in the temporal lobe, postcentral gyrus, thalamus, and occipital lobes (e.g., cluster 1 in Fig. 4A, and cluster 12 in Fig. 4B; also see Table 1). A large hyperperfusion cluster in the contralateral hemisphere (cluster 4 in Table 1) comprised frontal, parietal, temporal, and occipital cortex, and reflected the progressive involvement of the contralateral hemisphere as seizure severity increased. Three extratemporal lobe clusters (clusters 5, 8, and 9 in Fig. 4C,D; Table 1) showed hypoperfusion in early stage seizures, but hyperperfusion in stage IV seizures. For example, the cluster located in the ipsilateral frontal cortex corresponding to somatosensory and primary motor cortex of monkey S (Fig. 4C, cluster 5 in Table 1) showed a marked but gradual increase in perfusion by >50%, with the largest increase occurring between stage III and stage IV. In contrast, two other clusters located bilaterally in parietal cortex (Fig. 4D) showed hypoperfusion in stages I–III, which changed little in these stages, followed by a remarkable hyperperfusion in stage IV. We also observed clusters of voxels that showed progressively more hypoperfusion during the kindling process in prefrontal (Fig. 4E), temporal, and cingulate cortex, and several clusters in the cerebellum (Fig. 4F, clusters 18 and 19 in Table 1). Overall, SISCOM imaging revealed extensive changes in perfusion throughout the brain as seizure severity progressed during the course of amygdala kindling.

The clusters showing progressive hyperperfusion or hypoperfusion were identified based on the SISCOM images of stage IV, excluding the voxels of the common network. However, we noticed that half of the hyperperfusion clusters (6/12) and all of the hypoperfusion clusters were actually bordering or surrounded by clusters of the common network. The example in Figure 5A,B illustrates this observation for two hyperperfusion clusters. In addition, Figure S3A,B demonstrates the relationship between perfusion changes in the common network clusters and the hyperperfusion clusters. The examples shown illustrate two common network clusters that exhibited a constant level of hyperperfusion (green curve in Fig. S3A and yellow curve in Fig. S3B) and one common network cluster that showed an increase in perfusion from stage II on, while the surrounding cluster had the biggest increase in perfusion between stage III and IV (Fig. S3A yellow and red curve). The close relationship between progressive changes in perfusion and the nodes of the common network was even more apparent for the hypoperfusion clusters, as illustrated in Fig. 5C,D. We found that some common network nodes that are encircled by the hypoperfusion clusters exhibited parallel perfusion changes with these hypoperfusion clusters (Fig. S3C,D). These results demonstrate that changes in brain perfusion measured during the prolonged kindling process in the rhesus monkey originated largely from regions that were already implicated in seizure generation at stage I and that these regions do not necessarily show the same progression in perfusion changes.

Discussion

We electrically kindled the amygdala in two rhesus monkeys over >300 sessions. Both animals progressed from stage I (sub)clinical seizures of short duration with minimal behavioral signs to stage IV seizures of longer duration and bilateral motor signs over the course of 6–9 months. Partially originating from a network of regions that showed perfusion changes at every seizure stage (i.e., the common network), the perfusion changes progressively expanded to include larger brain regions in parallel with the clinical signs.

We essentially replicated the kindling results obtained by Wada et al.[5] in the rhesus monkey. Extending their work, we also implemented a behavioral task to assess the postictal period, and video-EEG to allow an objective assessment of seizure severity and duration. Although both animals experienced marked clinical symptoms in stage IV, the postictal period was relatively short (<30 s). A possible

Table 1. Overview of brain areas that showed a progressive increase (top) or decrease (bottom) in perfusion during kindling epileptogenesis

	Tentative anatomic localization	Side	Number of voxels	Monkey	% Perfusion change w.r.t. baseline perfusion			
					Stage I	Stage II	Stage III	Stage IV
Progressive hyperperfusion clusters								
Temporal cortex								
1	Temporal pole – premotor cortex – anterior insula	I	2,359	S	20.54	32.49	33.17	39.68
2	Anterior insula – putamen – premotor cortex	C	2,944	S	20.38	19.58	22.21	32.52
3	Anterior temporal cortex	C	243	K	23.13	23.27	37.26	51.77
Postcentral gyrus								
4	Primary motor cortex – somatosensory cortex – temporal areas (auditory cortex, STS) – parietal cortex (area 7) – midbrain – visual areas V1–V4	C	27,524	S	9.82	8.22	11.97	36.17
5	Somatosensory cortex (areas 1, 2, 3a/b) – primary motor cortex	I	1,119	S	−5.50	8.46	17.28	48.69
6	Somatosensory cortex (1–2, 3a/b) – premotor cortex – auditory temporal cortex	I	3,427	K	28.87	26.90	36.00	58.14
Subcortical structures								
7	Thalamus – ipsilateral dorsal insula to posterior insula – ipsilateral fundus of the STS	B	7,735	K	14.20	20.39	22.66	29.16
Visual system								
8	Parietal area 7a to V4	C	1,499	S	−19.98	−8.91	−5.57	57.05
9	Parietal area 7a to V4	I	2,513	S	−22.01	−19.13	−14.06	50.13
10	Visual areas V1–ventral V4	I	2,973	S	19.59	18.79	21.42	33.89
11	Visual area V2	I	567	S	4.72	8.86	14.72	24.99
12	Area TEO – V4	I	824	K	15.39	29.00	46.89	54.16
Progressive hypoperfusion clusters								
Prefrontal cortex								
13	Anterior prefrontal cortex Dorsolateral prefrontal cortex	C I	3,919	S	−12.24	−13.47	−24.80	−29.25
Temporal cortex								
14	Insula – temporal pole – putamen	I	2,724	K	−10.15	−10.23	−9.64	−19.95
15	Temporal area TE, fundus STS	I	1,232	K	−16.91	−16.83	−16.24	−22.09
Cingulate cortex								
16	Midline posterior cingulate – medial parietal cortex (area 7 m)	I	1,679	K	−14.28	−13.82	−21.28	−21.88
Cerebellum								
17	Cerebellar hemisphere – vermis	B	2,695	S	−13.43	−14.05	−16.83	−22.17
18	Cerebellar hemisphere	I	2,735	S	−1.45	−6.20	−11.33	−31.32
19	Cerebellar hemisphere	C	2,529	S	−14.98	−14.70	−19.95	−25.85
20	Cerebellar hemisphere and deep nuclei – bilateral superior colliculus – ipsilateral visual areas V1–V2	C	8,123	K	−10.12	−16.41	−16.90	−21.56

I, ipsilateral to stimulation side; C, contralateral; STS, superior temporal sulcus.

explanation for the failure to elicit seizures after 8–10 months of daily stimulation is the formation of a small lesion at the electrode tip, not detectable with MRI.[16] After electrical kindling was resumed with new electrodes, the animals quickly returned to stage IV, which means that the seizure-induced epileptogenetic changes had not been reversed.

Our study is the first study that investigates how the epileptic network changes over time in the amygdala kindling model in rhesus monkeys, using the same imaging techniques that are being used in humans. One of the major advantages of using a nonhuman primate model compared to human studies is the availability of imaging data of the naive brain. On the other hand, our experiments also had their limitations. First, we could not take into account possible interictal perfusion changes during the different seizure stages. Furthermore, because we used only two monkeys, grouped perfusion data to calculate the statistical significance of the changes we observed were not possible. Because of the overt limb

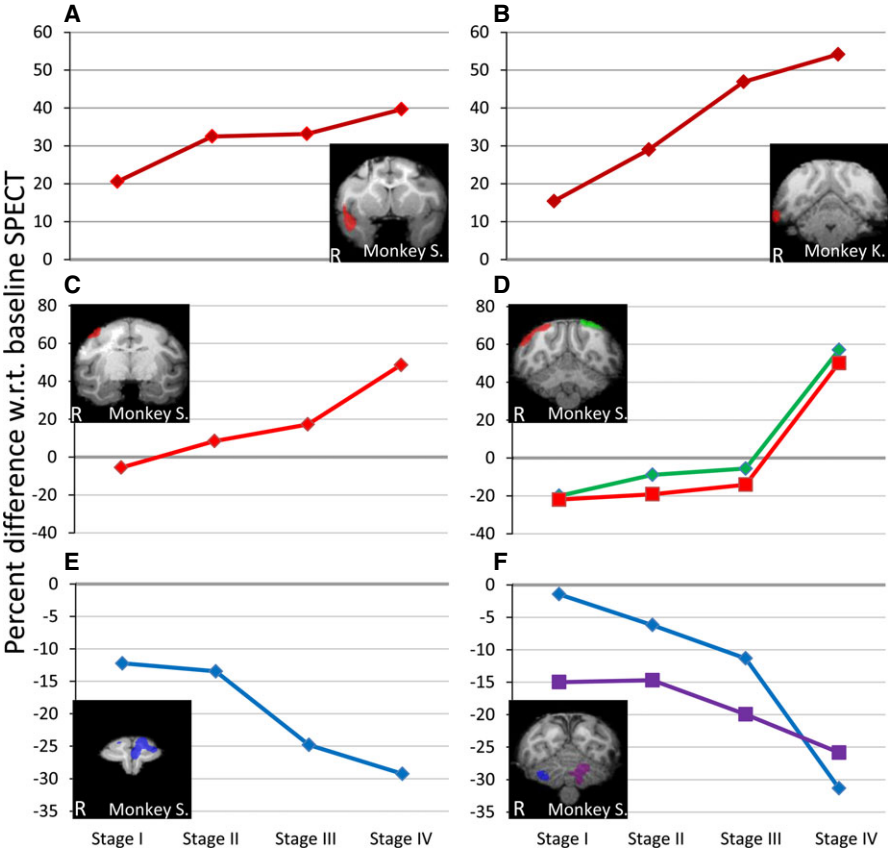

Figure 4.
Progressive changes in perfusion during kindling. (**A**, **B**) Examples of functionally defined clusters that show a progressive increase in perfusion with respect to the baseline SPECT scan over the course of kindling. (**C**, **D**) Clusters showing an initial hypoperfusion followed by hyperperfusion during kindling. (**E**, **F**) Clusters showing progressive hypoperfusion during kindling. Percent changes are depicted in Table 1. (**A**) Cluster 1 (monkey S). (**B**) Cluster 12 (monkey K). (**C**) Cluster 5 (monkey S). (**D**) Clusters 8 (green) and 9 (red) (monkey S). (**E**) Cluster 13 (monkey S). (**F**) Clusters 18 (blue) and 19 (purple) (monkey S). Same conventions as in Figure 2.

movements, the tracer injection had to take place at least 10 s before seizure onset. When taking into account the kinetics of ^{99m}Tc-ECD in the monkey brain,[14] we noted that most of our imaging results reflected the status of brain perfusion during the first part of the seizure. This latter limitation, however, may have led only to an underestimation of the changes in brain perfusion in the course of the kindling process. Moreover, a previous study measuring cerebral blood flow autoradiographically in fully kindled rats demonstrated that the hyperperfusion pattern was similar when injection occurred 30 s before or at the time of seizure induction.[17] Despite these limitations, we measured progressive changes in hyperperfusion that were related to the progression of clinical signs (e.g., motor cortex involvement–motor signs).

One of our most surprising findings was the observation of distributed perfusion changes common to all seizure stages and not confined to the stimulation site. The existence of a distributed common network implies that at least part of the network involved in seizure progression is already implicated before any clinical signs of epileptic seizures can be observed. Our data are in agreement with the observations of Chassagnon et al.,[18] who found a high number of hyperperfused (sub)cortical structures early in the course of amygdala kindling process in rats. Importantly and in contrast to these autoradiography studies in rats, we could perform in vivo measurements in the same animals over different seizure stages. Note that hyperperfusion was not always seen in the stimulated amygdala itself, especially in monkey K, which is consistent with previous autoradiographic studies in rats.[17,19]

A second major finding was the observation of three types of expansion over time that frequently originated from nodes of the common network as seizure severity increased. The first type was a hyperperfusion cluster that expanded over the different seizure stages, probably constituting the primary epileptic network. The second type was a cluster of hypoperfusion in the early stages, which became hyperperfused in later seizure stages. These clusters represent brain regions that became involved in the epileptic network at a later stage, for example, frontoparietal cortex. The third type was a cluster of hypoperfusion that became larger and more hypoperfused as seizures progressed, for example, in prefrontal cortex and cerebellum. Brain regions that are progressively recruited during kindling may represent potential targets for inhibiting seizure propagation using deep brain stimulation.[20] Alternatively, the network implicated in epileptogenesis may be so distributed that manipulation of brain activity in a single node may not suffice to reduce seizure propagation.

The common network we identified differed between the two animals in this study. This interindividual variability in

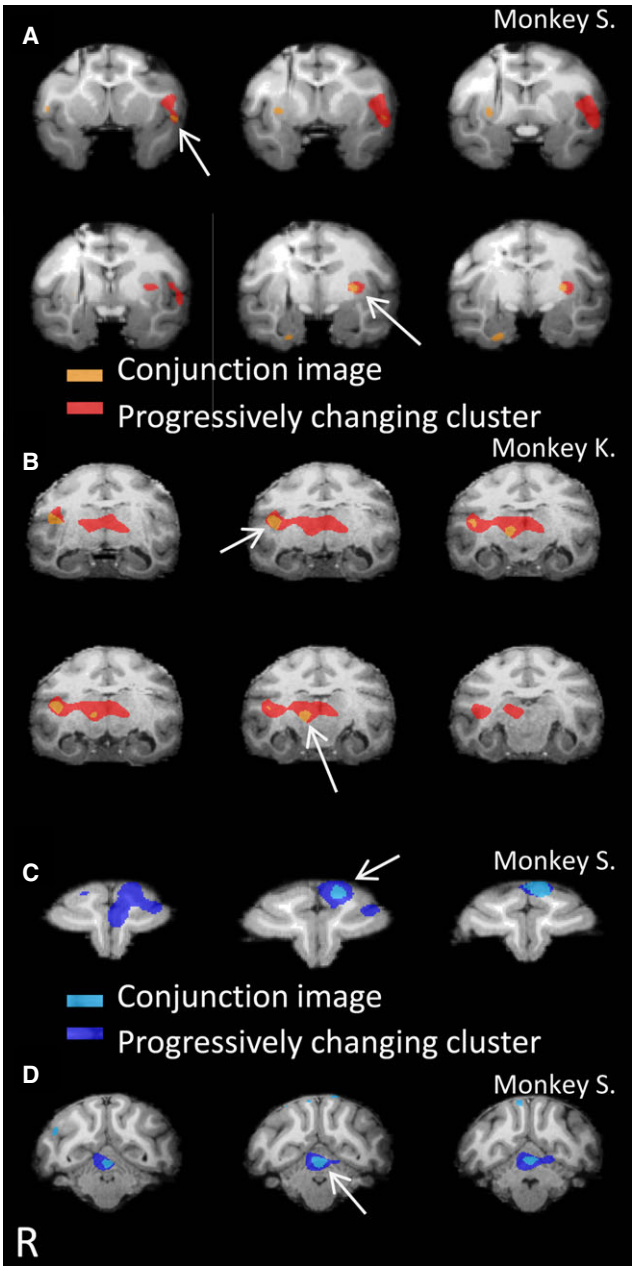

Figure 5.
Expansion of perfusion changes with respect to the common network. (**A**, **B**) Examples of functionally defined clusters showing a progressive increase (illustrated in red) in perfusion changes with respect to the baseline SPECT scan over the course of kindling. The conjunction image is shown in orange (hyperperfusion) to illustrate the expansion of the perfusion areas over time. (**A**) Cluster 2 (Table 1) illustrates this observation for a hyperperfusion cluster in the contralateral hemisphere of monkey S. Two nodes of the common network (i.e., already implicated in seizure activity from stage I onwards) were located in the contralateral temporal cortex and putamen. In stage IV, the region showing hyperperfusion had markedly expanded such that it included most of the lateral fissure, part of the insula and a larger portion of the putamen. (**B**) Cluster 7 shows another hyperperfusion cluster (in monkey K) originating in the lateral fissure and thalamus of the ipsilateral hemisphere (i.e., the nodes of the common network), which expanded to include a large part of the ipsilateral and even the contralateral thalamus in stage IV. (**C**, **D**) Examples of clusters that showed a progressive decrease (blue) in perfusion in monkey S. Conjunction image is shown in cyan. Cluster 13 (**C**) in the contralateral prefrontal cortex and cluster 17 (**D**) in the cerebellum: in both cases, the node of the common network was located at the center of the hypoperfusion cluster, indicating progressive expansion of the hypoperfusion region in the course of the kindling process. Same conventions as in Figure 2.

the common network can be expected in view of the diverse anatomic connectivity of the various nuclei within the amygdala[21] and slight differences in the anatomic locations of the stimulation electrodes in the two animals. Furthermore, also in TLE patients, the networks involved can be highly diverse.[22] Thus, despite the between-animal differences we observed, our main findings were clearly replicated in both subjects.

The macaque monkey amygdala kindling model exhibited unique features that are directly relevant for the study of neural alterations associated with human temporal lobe epileptogenesis. First, seizure severity and duration in the amygdala kindling model in the rhesus monkey progressed slowly, just as in human MTLE.[23] Second, we were not able to elicit symmetric generalized tonic–clonic seizures (GTCS) in our animals. It remains to be explored whether this type of seizure could be elicited with longer kindling periods. Likewise, in human MTLE, secondary GTCS are never the predominant seizure type, and tend to occur later in the disease progression.[23] Third, seizure semiology in our model was in many ways comparable with human MTLE seizures. Fourth, we were able to monitor and visualize our animals using the same imaging techniques employed with humans.[12,24–26] In contrast to human studies, all seizures in our study occurred in a highly controlled environment, and baseline measurements of the naive brain allowed a direct assessment of changes in brain perfusion.

It could be argued that the amygdala kindling model is not adequate for epilepsy because the animals never develop spontaneous seizures and seizures have to be elicited by artificial electrical stimulation. However, understanding the neural basis of epileptogenesis requires charting the changes in the network of cortical and subcortical structures that occur as seizure severity increases over time. With this objective, the primary cause of epileptic activity (trauma, infection, dysplasia, hippocampal sclerosis, or electrical stimulation) may be less important, since the network involved in epileptogenesis is remote from the seizure-onset zone in the amygdala. Our data suggest that controlling temporal lobe auras, which may correspond to stage I seizures, could prevent seizure-induced epileptogenesis. Future

studies can now investigate whatever molecular changes occur at these locations as a consequence of repeated epileptic seizures, so that the neural basis of epileptogenesis can be determined and adequate preventive strategies for epilepsy patients can be developed.

Acknowledgments

Supported by the Fund for Scientific Research Flanders (G.0745.09) and the Programma Financiering (PFV/10/008). The authors thank Ann Van Santvoort, Kwinten Porters, Peter Vermaelen, and Johan Nuyts, as well as the Leuven PET radiopharmacy team. We thank Steve Raiguel for comments on a previous version of this manuscript. Technical assistance of Christophe Ulens, Piet Kayenbergh, Gerrit Meulemans, Jan Lenaerts, Stijn Verstraeten, Wouter Depuydt, Marc De Paep, Astrid Hermans, Inez Puttemans, and Sara De Pril is greatly acknowledged.

Disclosure

None of the authors has any conflict of interest to disclose. All authors confirm to have read the Journal's position on issues involved in ethical publication and affirm that this report is consistent with those guidelines.

References

1. Tellez-Zenteno JF, Hernandez-Ronquillo L. A review of the epidemiology of temporal lobe epilepsy. *Epilepsy Res Treat* 2012;2012:630853.
2. Bertram E. The relevance of kindling for human epilepsy. *Epilepsia* 2007;48 (Suppl. 2):65–74.
3. Pitkanen A, Schwartzkroin PA, Moshé SL. *Models of seizures and epilepsy*. Burlington, MA: Elsevier Academic Press; 2006.
4. Wada JA, Osawa T. Spontaneous recurrent seizure state induced by daily electric amygdaloid stimulation in Senegalese baboons (*Papio papio*). *Neurology* 1976;26:273–286.
5. Wada JA, Mizoguchi T, Osawa T. Secondarily generalized convulsive seizures induced by daily amygdaloid stimulation in rhesus monkeys. *Neurology* 1978;28:1026–1036.
6. Wada JA, Mizoguchi T, Komai S. Kindling epileptogenesis in orbital and mesial frontal cortical areas of subhuman primates. *Epilepsia* 1985;26:472–479.
7. Ribak CE, Seress L, Weber P, et al. Alumina gel injections into the temporal lobe of rhesus monkeys cause complex partial seizures and morphological changes found in human temporal lobe epilepsy. *J Comp Neurol* 1998;401:266–290.
8. Devergnas A, Piallat B, Prabhu S, et al. The subcortical hidden side of focal motor seizures: evidence from micro-recordings and local field potentials. *Brain* 2012;135:2263–2276.
9. Goddard GV. Development of epileptic seizures through brain stimulation at low intensity. *Nature* 1967;214:1020–1021.
10. Cain DP. Kindling and the amygdala. In Aggleton JP (Ed) *The amygdala: neurobiological aspects of emotion, memory, and mental dysfunction*. New York: Wiley-Liss, Inc., 1992:539–560.
11. Newey CR, Wong C, Wang ZI, et al. Optimizing SPECT SISCOM analysis to localize seizure-onset zone by using varying z scores. *Epilepsia* 2013;54:793–800.
12. Van Paesschen W, Dupont P, Van Driel G, et al. SPECT perfusion changes during complex partial seizures in patients with hippocampal sclerosis. *Brain* 2003;126:1103–1111.
13. Laufs H, Rodionov R, Thornton R, et al. Altered fMRI connectivity dynamics in temporal lobe epilepsy might explain seizure semiology. *Front Neurol* 2014;5:175.
14. Walovitch RC, Hill TC, Garrity ST, et al. Characterization of technetium-99m-L, L-ECD for brain perfusion imaging, Part 1: pharmacology of technetium-99m ECD in nonhuman primates. *J Nucl Med* 1989;30:1892–1901.
15. O'Brien TJ, O'Connor MK, Mullan BP, et al. Subtraction ictal SPET co-registered to MRI in partial epilepsy: description and technical validation of the method with phantom and patient studies. *Nucl Med Commun* 1998;19:31–45.
16. Goddard GV, McIntyre DC, Leech CK. A permanent change in brain function resulting from daily electrical stimulation. *Exp Neurol* 1969;25:295–330.
17. Chassagnon S, de Vasconcelos AP, Ferrandon A, et al. Time course and mapping of cerebral perfusion during amygdala secondarily generalized seizures. *Epilepsia* 2005;46:1178–1187.
18. Chassagnon S, Andre V, Koning E, et al. Optimal window for ictal blood flow mapping. Insight from the study of discrete temporo-limbic seizures in rats. *Epilepsy Res* 2006;69:100–118.
19. Engel J Jr, Wolfson L, Brown L. Anatomical correlates of electrical and behavioral events related to amygdaloid kindling. *Ann Neurol* 1978;3:538–544.
20. Fridley J, Thomas JG, Navarro JC, et al. Brain stimulation for the treatment of epilepsy. *Neurosurg Focus* 2012;32:E13.
21. Zhang W, Schneider DM, Belova MA, et al. Functional circuits and anatomical distribution of response properties in the primate amygdala. *J Neurosci* 2013;33:722–733.
22. Ho SS, Berkovic SF, McKay WJ, et al. Temporal lobe epilepsy subtypes: differential patterns of cerebral perfusion on ictal SPECT. *Epilepsia* 1996;37:788–795.
23. French JA, Williamson PD, Thadani VM, et al. Characteristics of medial temporal lobe epilepsy: I. Results of history and physical examination. *Ann Neurol* 1993;34:774–780.
24. Shin WC, Hong SB, Tae WS, et al. Ictal hyperperfusion of cerebellum and basal ganglia in temporal lobe epilepsy: SPECT subtraction with MRI coregistration. *J Nucl Med* 2001;42:853–858.
25. Shin WC, Hong SB, Tae WS, et al. Ictal hyperperfusion patterns according to the progression of temporal lobe seizures. *Neurology* 2002;58:373–380.
26. Spencer SS. Neural networks in human epilepsy: evidence of and implications for treatment. *Epilepsia* 2002;43:219–227.

Supporting Information

Additional Supporting Information may be found in the online version of this article:

Figure S1. EEG traces.

Figure S2. Epidural EEG changes during stage I (monkey S).

Figure S3. Perfusion changes in the common network in relationship with the expanding perfusion network.

Data S1. Methods.